Published in final edited form as:
Biosens Bioelectron. 2011 April 15; 26(8): 3577–3583. doi:10.1016/j.bios.2011.02.004.

Ternary Monolayers as DNA Recognition Interfaces for Direct and Sensitive Electrochemical Detection in Untreated Clinical Samples

Susana Campuzano[a], **Filiz Kuralay**[a], **M. Jesús Lobo-Castañón**[a], **Martin Bartošík**[b], **Kedar Vyavahare**[a], **Emil Paleček**[b], **David A. Haake**[c,d], and **Joseph Wang**[a,*]

[a]Department of Nanoengineering, University of California San Diego, La Jolla, CA 92093, USA

[b]Institute of Biophysics, Academy of Sciences of the Czech Republic, Brno, Czech Republic, University of California Los Angeles

[c]Institute of Biophysics, Department of Medicine, David Geffen School of Medicine at University of California Los Angeles, Los Angeles, CA 90095, USA

[d]Veterans Affairs Greater Los Angeles Healthcare System, Los Angeles, CA 90073

Abstract

Detection of specific DNA sequences in clinical samples is a key goal of studies on DNA biosensors and gene chips. Herein we present a highly sensitive electrochemical genosensor for direct measurements of specific DNA sequences in undiluted and untreated human serum and urine samples. Such genosensing relies on a new ternary interface involving hexanedithiol (HDT) co-immobilized with the thiolated capture probe (SHCP) on gold surfaces, followed by the incorporation of 6-mercapto-1-hexanol (MCH) as diluent. The performance of ternary monolayers prepared with linear dithiols of different lengths was systematically examined, compared and characterized by cyclic voltammetry and electrochemical impedance spectroscopy, with HDT exhibiting the most favorable analytical performance. The new SHCP/HDT+MCH monolayer led to a 80-fold improvement in the signal-to-noise ratio (S/N) for 1 nM target DNA in undiluted human serum over the common SHCP/MCH binary alkanethiol interface, and allowed the direct quantification of the target DNA down to 7 pM (28 amol) and 17 pM (68 amol) in undiluted/untreated serum and urine, respectively. It also displayed attractive antifouling properties, as indicated from the favorable S/N obtained after a prolonged exposure (24 h) to untreated biological matrices. These attractive features of the SHCP/HDT+MCH sensor interface indicate considerable promise for a wide range of clinical applications.

Keywords

Dithiols; self-assembled monolayer; clinical samples; electrochemical detection; hybridization; DNA

*To whom correspondence should be addressed. josephwang@ucsd.edu., Fax: +1 858-534-9553. .

1. Introduction

There is a considerable interest in development of simple and highly sensitive techniques for detecting specific DNA sequences in complex biological matrices such as serum and urine. Electrochemical detection of DNA hybridization couples high sensitivity and simplicity with low cost, portability and low power requirements. Current efforts aimed at detecting nucleic acids in complex biological matrices without PCR amplification, at minimizing background contributions and improving the reproducibility should facilitate routine genoassays of human diseases. Although the detection limit of electrochemical sensors for target DNA has been greatly improved over the past few years (Arya et al., 2009; Batchelor-McAuley et al., 2009; Miranda-Castro et al., 2009; Sadik et al., 2009; Sassolas et al., 2008; Wang, 2006), the determination of a single copy of a specific nucleic acid sequence in biological fluids without PCR amplification remains a challenging task. Another major challenge is the detection of the probe-target duplex in presence of a large excess of non-complementary human DNA. Typically, hybridization of the capture probe with the complementary target sequence is performed in hybridization buffers, where interferences of other biomolecules are minimized (Tosar et al., 2010). However, in biological matrices, like urine or serum, the target DNA is present along with a large amount and variety of biomolecules including, but not limited to non-target DNA molecules, proteins, carbohydrates, etc., which may cause undesired interferences in measured responses. For instance, electroactive interferences may lead to overlapping signals and to false (positive) result. Similarly, if the interfering molecule blocks the surface via a nonspecific adsorption, it can greatly diminish the hybridization efficiency, leading to a lower (false negative) response. Applications of electrochemical DNA sensors in pure untreated biological matrices have been very limited. In cases when a biological matrix is used, a 10-fold dilution is usually performed (Das et al., 2010; Patterson et al., 2010; Zhang et al., 2008). Very recently, trace nanomolar detection of DNA was carried out in 1:1 diluted serum samples (Xia et al., 2010; Pei et al., 2010). To our knowledge, direct measurement of DNA in undiluted biological matrices has not been reported.

Here we report for the first time how a judicious interfacial design allows the direct measurement of DNA sequences in undiluted human serum and urine samples. The new surface design involves the use of hexanedithiol (HDT) co-immobilized with thiolated capture probe at gold surfaces by chemisorption along with MCH as diluent. The sensor interface plays a crucial role in the overall performance of electrochemical genosensors. Nonspecific adsorption effects, a major challenge in clinical matrices, can be reduced by employing mixed self-assembled monolayers (SAMs) containing a thiol-derivatized capture probe DNA and a spacer thiol, mainly MCH (Steel et al., 1998). These mixed SAMs also improve the reproducibility and hybridization efficiency (Keighley et al., 2008; Lao et al., 2005; Levicky et al., 1998). Yet, such binary monolayers still suffer from background contributions and irreproducibility problems resulting from incomplete backfilling and surface defects (Boozer et al., 2006; Keighley et al., 2008; Lao et al., 2005). The challenges associated with binary layers have been recently addressed by introducing a third thiol component (Dharuman et al., 2010; Dharuman and Hahn, 2008; Wu et al., 2010). For example, a ternary layer formed by co-immobilizing the cyclic dithiol dithiothreitol (DTT) with the SHCP, followed by sequential addition of MCH, offered recently efficient hybridization and high resistance to non-specific adsorption effects to facilitate measurements in diluted human serum (25%), along with ultrasensitive detection in pure hybridization buffer (Wu et al., 2010). To achieve even better S/N characteristics and improved the performance in undiluted clinical samples, compared to the DTT ternary interface, we have examined and compared in the present study linear dithiols of different lengths as the third interfacial component (Fig. 1). The selected SHCP/HDT+MCH interface is shown in the following sections to offer both high hybridization efficiency and remarkable

antifouling capability, resulting in measurements of pM target concentrations in undiluted clinical samples. Relations between the structure of these linear dithiols and the analytical performance of the ternary monolayers have been systematically evaluated. In undiluted human serum the HDT-based ternary SAM layer offered 80-fold and 8-fold improvements in the S/N over the common binary and the recently reported DTT ternary layers, respectively. As will be illustrated below, this bioplatform also displays favorable non-fouling properties after 24 h immersion in the selected clinical samples. Such capabilities offer great promise for practical bioanalytical applications.

2. Materials and methods

2.1. Materials

6-mercapto-1-hexanol (MCH, 97%), 1,3-propanedithiol (PDT, 99%), 1,6-hexanedithiol (HDT, 96%), 1-hexanethiol (HMT, 95%), 1,9-nonanedithiol (NDT, 95%), DL-dithiothreitol (DTT), Trizma hydrochloride (Tris-HCl), ethylenediaminetetraacetic acid (EDTA), human serum (from human male AB plasma) and bovine serum albumin (BSA) were obtained from Sigma-Aldrich (St. Louis, MO) and used without further purification. The blocking agent casein was obtained from Pierce (Rockford, IL). The enzyme substrate 3,3′,5,5′-tetramethylbenzidine (TMB, Neogen K-blue enhanced activity substrate, containing H_2O_2) was obtained from Neogen (Lexington, KY). The conjugated anti-fluorescein-horseradish peroxidase (anti-FITC-HRP, Fab fragments) was purchased from Roche Diagnostics (Mannheim, Germany).

The composition of the buffers used in the different experimental steps was as follows: the immobilization buffer (IB) contained 10 mM Tris-HCl, 1 mM EDTA, and 0.3 M NaCl (pH 8.0), the hybridization buffer (HB) was a 1.0 M phosphate solution containing 2.5% BSA (pH 7.2), and the binding buffer (BB), for the incorporation of the conjugated anti-FITC-HRP, consisted of PBS (1×) containing 0.5% casein (pH 7.2).

All synthetic oligonucleotides used, designed for detecting a characteristic region of *E. coli* 16S rRNA, were purchased from Integrated DNA Technologies, Inc. (CA, USA) and are listed in Table S-1 of the Supporting Information.

2.2. Instrumentation

Chronoamperometric measurements were performed on disposable 16-sensor Au electrode arrays (GeneFluidics Inc. Monterey Park, CA, USA). Each sensor consisted of a 2.5 mm diameter central gold working electrode, surrounded by a gold counter electrode and a gold pseudo-reference electrode. The sensor chip was driven by a computer-controlled PalmSens hand-held potentiostat with an eight-channel PalmSens Multiplexer (Palm Instruments BV, Houten, The Netherlands).

Cyclic voltammetry (CV) and electrochemical impedance spectroscopy (EIS) were performed with a CHI 660D Electrochemical Analyzer (CH Instruments, Austin, TX, USA). These experiments were undertaken using a conventional three-electrode setup with a 2 mm diameter gold disk (AuE) as working electrode, a Ag/AgCl reference electrode and a Pt wire as auxiliary electrode. Previously described pretreatment procedure was used to clean the working electrode (Campuzano et al., 2002). The measurements were carried out in a 0.1 M KCl solution containing 5 mM of $K_3Fe(CN)_6$ and 5 mM of $K_4Fe(CN)_6$. Electrochemical impedance spectra were obtained at +0.25 V under an AC amplitude of 0.01 V and a frequency range from 0.01 to 10,000 Hz. The impedance data were analyzed by non-linear least-squares using the EQUIVCTR.PAS (EQU) program by Boukamp.

2.3. Procedures

2.3.1. Preparation of DNA recognition interfaces—A mixture of SHCP and a freshly prepared dithiol, with appropriate concentrations, was prepared in IB buffer and allowed to stand for 10 min. Aliquots of 6 μL of this mixture were cast over each Au working electrode in the 16-sensor array and incubated overnight at 4 °C in a humidified chamber. After washing with water and drying with nitrogen, the mixed monolayer-modified Au sensors were subsequently treated with 6 μL of 1 mM MCH aqueous solution (in IB buffer) for 50 min to obtain the ternary SAM interfaces. Finally, the sensors were thoroughly rinsed with water and dried under nitrogen.

2.3.2. DNA hybridization assay in HB—The sensor response was evaluated with a sandwich-type hybridization assay, using fluorescein as a tracer in the detection probe and anti-fluorescein-HRP as the reporter molecule. TMB was the selected substrate for the electrochemical measurement of the activity of the captured HRP reporter. Different concentrations of the target DNA were mixed with FITC-DP (0.25 μM) in HB and allowed to react for 15 min for homogeneous hybridization. Aliquots of 4 μL of the preformed hybrid solution were cast on each of the SAM-modified gold sensors and incubated for 15 min. After hybridization, the array was washed and dried and each working electrode in the array was incubated with 4 μL of a 0.5 U mL^{-1} anti-FITC-HRP solution in BB for 15 min. Subsequently, the array was washed and dried, and a prefabricated plastic 16-well manifold (GeneFluidics, Monterey Park, CA, USA) was bonded to the sensor array. To perform the chronoamperometric detection, 50 μL of the TMB–H_2O_2 K-Blue reagent solution were placed sequentially on each of the sensors in the array, covering the three electrodes area. After 30 s, the potential was stepped to −200 mV (vs. the gold pseudo-reference electrode) and the current was sampled during 60 s.

2.3.3. DNA hybridization assay in clinical samples and non-fouling properties —In this case, HB was substituted for the clinical sample under study; both target DNA and FITC-DP (0.25 μM) were prepared directly either in undiluted commercial human serum or fresh untreated urine. The homogeneous hybridization between different target concentrations and the detection probe was carried out in the untreated samples and then 4 μL of the hybrid solution were cast on each modified sensor and incubated for 15 min. The following steps: capture of anti-FITC-HRP and electrochemical detection were carried out using the same protocol described above for the determination of target DNA in HB. All procedures were carried out at room temperature (22-25 °C).

For the evaluation of the non-fouling properties of the new interfaces, a 6 μL droplet of the untreated clinical samples was cast over each SAM-modified working electrode and left overnight at 4 °C in a humidified surrounding. After washing with water and drying with nitrogen, the sensor array was used for the determination of target DNA in HB as mentioned above.

3. Results and discussion

3.1. Comparison of different interfaces and design of the dithiols-based ternary SAMs

Different DNA sensing interfaces were prepared in a two-step procedure by co-assembling the SHCP and a dithiol (PDT, HDT or NDT) onto the gold electrode followed by the incorporation of the MCH diluent. The hybridization efficiency of these interfaces was determined by chronoamperometric measurements using the sandwich hybridization assay described before. Fig. 2 and Table S-2 compare current signals obtained in the presence and absence of 1 nM of target DNA, along with the resulting S/N ratios for the different layers tested. Common binary layer displayed large background current, suggesting high

susceptibility to nonspecific adsorption. As a consequence, a low S/N ratio, which hinders the detection of low levels of target DNA, even in pure HB, is obtained at the binary interface. Considerably higher S/N ratio - for the same target DNA concentration – is observed using the SHCP/DTT+MCH ternary layer, due to greatly suppressed background current. However, co-immobilization of DTT also caused a ~2.5 fold decrease of the resulting signal as compared to binary layer (3344.4 vs 1364.1 nA, Table S-2), probably due to a high surface compactness that hinders the permeability of the enzymatic product. Interestingly, when PDT and HDT were used as backfillers, the current response of 1 nM target DNA was restored back to the values of binary layer, while keeping the noise at the level of DTT ternary layer. Thus, S/N values reached 333.6 and 344.9 for SHCP/PDT+MCH and SHCP/HDT+MCH ternary layers, respectively. Use of NDT as a backfiller also improved the S/N value (217.1), though to a somewhat lesser degree than PDT and HDT. These results demonstrate that monolayers prepared from linear dithiols with lengths between 3 and 6 carbon atoms exhibit the most favorable analytical performance. The S/N characteristics obtained for the different SAM interfaces, clearly indicate that the presence of a 3rd component, its structure and adopted configuration during the assembly are key contributors to the remarkable non-fouling properties of the new layers. On the other hand, the fabrication of the layers following co-assembling or sequential assembly processes and the length of the 3rd component contribute primarily to the signal but have only a slight effect upon the background current.

The improved performance of PDT- and HDT-based ternary surfaces over DTT-based ternary surfaces can be attributed to the preferential lying-down orientation adopted by these linear dithiols under the experimental conditions used that minimizes nonspecific adsorption of proteins and other biomolecules (leading to low noise, similar to that obtained with DTT), while maintaining favorable orientation of the capture probe and good permeability of small molecules, such as the TMB signaling one, hence leading to higher signals. We assume that at the concentrations used, the linear dithiols examined here are mostly lying flat on the surface with the two thiol groups chemisorbed onto the gold (Fig. 1). In this way, these molecules could act as bridges over certain surface irregularities, leading to monolayers with high stiffness and directionality. Consistent with this, we found that ternary monolayers using HMT instead of HDT display a similar behavior to that of binary monolayers i.e. a higher noise level and lower S/N ratio (Supporting Information Fig. S-1 and Table S-2), which is consistent with the upright configuration of the monothiol. In contrast, as seen in Table S-2, a binary monolayer of SHCP/HDT led to low noise but also to a very low signal. In the new ternary surfaces, the main role of the MCH seems to provide a standing-up configuration of the SHCP, with improved orientation and hybridization efficiency. In the case of SHCP/DTT monolayers the signal, but also the noise were high. Therefore, it seems that DTT is able to orient the SHCP in a position favorable for the hybridization, but MCH is required to reduce the noise. These results allow us to conclude that the use of a linear or cyclic dithiol co-assembled previously with the SHCP determine a different role of the third component of the layer, the MCH. According with the results achieved, cyclic dithiols like DTT are able to orient the SHCP for high hybridization efficiency but require MCH for minimizing the background current. Although it is expected that longer dithiols, like HDT (in their upright configuration), should promote stand-up of the capture probe, the results obtained (mainly by the comparison with the performance of the SHCP/HMT+MCH layer) support the hypothesis that under the selected experimental conditions, HDT adopts a lying down configuration but requires MCH to orient the SHCP in the upright position. Such lying down configuration of the HDT is in agreement with an earlier report (Leung et al., 2000).

3.2. Optimization of the co-assembled SHCP/dithiols SAMs

The surface coverage and the spacing of the SHCP molecules are dependent on the concentration of the co-immobilized dithiol component. One can assume a dynamic competition between -SH groups of SHCP and the dithiol backfillers, until equilibrium (governed by the actual concentrations of the competing molecules) is established. Under the optimum dithiol concentration, a tradeoff between the surface density, brought about by addition of the dithiols, and the hybridization efficiency (related to the SHCP surface coverage) is such that the best S/N characteristics is achieved. This is indeed the case also in our ternary layer design (Fig. S-2). Using low concentrations of any backfiller component, high nonspecific adsorption - due to incomplete surface coverage - led to a higher noise, and thus to lower S/N values. On the other hand, relatively high concentrations of the dithiols (> 300 μM) could displace some of the capture probe molecules, decreasing the hybridization efficiency, and hence the resulting signal and the S/N. For NDT, the optimum concentration is around 200 μM, whereas for PDT and HDT it is around 300 μM. It should be pointed out that these optimal levels hold only if 0.05 μM SHCP and 1 mM MCH are used. Also note that the S/N values under the optimum dithiol concentrations are higher for HDT and PDT, and lower for NDT, in agreement with Fig. 2.

3.3. Electrochemical characterization of the ternary layer

A key factor for designing DNA recognition interfaces is to assess the quality of the created monolayer. The compactness and surface coverage of the designed ternary layers was estimated by CV and EIS, comparing their characteristics with those of commonly used binary monolayer. The results are illustrated in Fig. 3.

Firstly, the blocking effect of the SAMs was examined by CV using $[Fe(CN)_6]^{3-/4-}$ as a redox probe. As shown in Fig. 3A, after modifying the gold surface a decrease in the anodic and cathodic peak currents and an increase in the peak potential separation (ΔE_p) are observed when compared with the voltammetric behavior of bare Au surfaces. The interfacial electron-transfer between gold and bulk solution is blocked by the ternary layer in different extents depending on the structure of the backfiller, following the order: DTT > PDT > HDT ≈ NDT. It should be noted that ternary layers prepared with HDT and NDT show a blocking effect similar to the conventional binary monolayer.

The fractional coverage of the electrodes by different SAMs was determined by EIS which also allows evaluation of the structural integrity of the different monolayers. Fig. 3B shows Nyquist plots for bare Au electrodes (a) and for Au electrodes modified with binary SHCP +MCH (b) and the different ternary monolayers: SHCP/DTT+MCH (c), SHCP/PDT+MCH (d), SHCP/HDT+MCH (e), and SHCP/NDT+MCH (f). The bare electrode displays a diffusion-limited electrode process. In contrast, the electrodes modified with mixed monolayers showed a semicircular portion in the higher frequency range of the spectra, which corresponds to an electron transfer limited process. In the case of SHCP/DTT+MCH monolayer the low-frequency linear-mass transfer region was not observed because the electrode process is under kinetic control over the entire frequency range. Qualitatively, these results reveal increasing barrier properties of the ternary monolayer in the order DTT > PDT > HDT ≈ NDT, in accordance with the results obtained by CV. The modified Randles equivalent circuit (see inset in Fig. 3B) was used to model the EIS data and to determine the values of the circuit components (Park and Yoo, 2003): the electrolyte resistance (R_s), the electron transfer resistance (R_{et}), the Warburg impedance (Z_W) associated to mass-transport of the redox species to the electrode surface, and the double layer capacitance (Q). A constant phase element instead of a pure capacitor was used in this study to calculate the double layer capacitance in order to take into account the phenomenon of frequency dispersion of capacitance, often directly related to microscopic roughness of the electrode

surface (Piela and Wrona, 1995). These parameters are summarized in Table 1. The Nyquist plots clearly illustrate the increased electron transfer resistance value upon changing from a naked surface (1.0 kΩ), to the various ternary SAMs with the maximum R_{et} being 32.6 kΩ for the case of monolayer that include DTT.

The apparent fractional coverage of the electrode (θ_{IS}^{R}) can be estimated, according with equation 1, from the magnitude of the charge-transfer resistance of the modified electrode (R_{et}^{SAM}) and the charge transfer resistance of the uncoated electrode (R_{et}^{AuE}), assuming that the electron transfer reaction occurs only at bare surface spots and that diffusion to these defect sites is planar (Janek et al., 1998).

$$\theta_{IS}^{R} = 1 - \left(\frac{R_{et}^{AuE}}{R_{et}^{SAM}} \right) \quad (1)$$

The surface coverage follows the order: SHCP/DTT+MCH > SHCP/PDT+MCH > SHCP/HDT+MCH ≈ SHCP/NDT+MCH ≈ SHCP+MCH. These electrochemical characterization results are in agreement with the high signal obtained with PDT and HDT based ternary layers due to a better permeability of these monolayers in comparison with the compact and nearly complete surface coverage offered by the ternary DTT SAM. Since the barrier properties and the surface coverage (and hence the noise level) of HDT- and NDT-based ternary layers are similar, the different S/N characteristics clearly reflect differences in the signal due to the lower amount of thiolated capture probe on the NDT interface.

3.4. Electrochemical detection of DNA hybridization in complex biological samples

Serum and urine are complex biological samples with multiple components that can be adsorbed nonspecifically onto the sensing interface, interfering with the binding of the target DNA and/or increasing the background signal. We found that the new ternary recognition interfaces allow the direct detection of trace target DNA in pure human serum and urine. To the best of our knowledge, this represents the first report describing the detection of picomolar DNA concentrations in these matrices without previous dilution or pretreatment. As a first step toward this goal, we compared the chronoamperometric responses for 1 nM target concentration at the commonly employed SHCP+MCH binary interface (Steel et al., 1998; Steel et al., 2000) with those observed at the new HDT-based ternary layer in either 100% human serum or urine (Fig. 4 Top, A and 4B). It is important to note that the noise level observed when the ternary monolayers were incubated in undiluted human serum was even lower than that observed in HB. A higher background signal was obtained in pure urine. For example, the ternary SHCP/HDT+MCH surfaces gave rise to background signals of 5.6±0.9 nA and 15.7±0.7 nA in serum and urine, respectively. However, when the binary monolayer was employed the background signal dramatically increased, in such a way that it was not possible to measure even a 1 nM target DNA in these matrices. The SHCP/HDT +MCH ternary monolayer, in contrast, yielded high S/N for the 1 nM target in such media and was used for further characterization. Note the change in the current scale to illustrate the negligible background noise compared to the binary interface. The excellent resistance to fouling in complex matrices offered by the new ternary interfaces is of great relevance to real-world applications of genosensors. As illustrated in Fig. 4 (Bottom) and in Table S-3, despite the ~50% signal loss, a favorable S/N ratio is observed for 1 nM target DNA concentration (in HB) when the assay was performed over chips that were previously dipped for 24 h in 100% serum (Fig. 4 Bottom, A) and urine (Fig. 4 Bottom, B) samples.

To determine the detection limit of the new biointerface in undiluted clinical samples, the SHCP/HDT+MCH was exposed to different (pM) levels of the target DNA in 100% human

serum (Fig. 5A) and urine (Fig. 5B). As shown in Fig. 5, the chronoamperometric signal increased linearly with the concentration of target DNA up to 150 pM, with a detection limit of 7 pM (28 amol) in human serum and 17 pM (68 amol) in urine. The detection limit obtained with the HDT-ternary monolayer in undiluted clinical samples is notably lower than those reported previously for SAM-based electrochemical DNA sensors in diluted samples. For example, the detection limit of the new HDT-based monolayer is more than 10-fold lower than that reported recently in 50% serum (Pei et al, 2010).

This a attractive performance in undiluted clinical samples, along with the ability to reproducibly fabricate these interfaces (RSD of 12.4% for the S/N values obtained after hybridization with 1 nM of target DNA in HB with 10 different electrodes), indicate promise for routine real-life DNA sensing.

4. Conclusions

We report for the first time the design of a ternary self-assembled monolayer, composed of a SHCP, HDT, and MCH. This monolayer provides several attractive features that facilitate direct measurement of target DNA in undiluted and untreated human serum and urine samples. The high hybridization efficiency even in complex samples has been attributed to the favorable surface architecture. HDT may adopt a horizontal configuration, acting as a bridge over certain surface irregularities, thus providing significantly higher resistance to nonspecific adsorption of nucleic acids and proteins. The negligible noise and high signal obtained with this ternary monolayer allowed higher S/N and significantly improved analytical performance compared to the conventional binary monolayers. Despite of the use of untreated biological matrices, the new interface offers direct measurement of attomole (pM) levels of target DNA specific for *E. coli* pathogenic bacteria in serum or urine. In addition, this new bioplatform displayed excellent antifouling properties. Such attractive behavior offers great promise for further progress in the field of chip-based bioelectronic detection and for decentralized detection in areas such as clinical diagnostics, biodefense, forensic analysis, and food safety.

Supplementary Material

Refer to Web version on PubMed Central for supplementary material.

Acknowledgments

Financial support from the National Institutes of Health (Award U01 AI075565) is gratefully acknowledged. SC, MJLC and FK acknowledge fellowships from Programa Becas Complutense del Amo (2010-2011), University of Oviedo and Spanish Ministerio de Ciencia e Innovacion (PR 2009-0430), and The Scientific and Technical Council of Turkey (TUBITAK), respectively. EP and MB thank the Czech-Republic Ministry of Education, Youth and Sports (ME09038).

References

Amatore C, Saveant JM, Tessier D. J. Electroanal. Chem. 1983; 147:39–51.

Arya SK, Solanki PR, Datta M, Malhotra BD. Biosens. Bioelectron. 2009; 24:2810–2817. [PubMed: 19339167]

Batchelor-McAuley C, Wildgoose GG, Compton RG. Biosens. Bioelectron. 2009; 24:3183–3190. [PubMed: 19264472]

Boozer C, Chen SF, Jiang SY. Langmuir. 2006; 22:4694–4698. [PubMed: 16649784]

Campuzano S, Galvez R, Pedrero M, de Villena FJM, Pingarron JM. J. Electroanal. Chem. 2002; 526:92–100.

Das J, Lee JA, Yang H. Langmuir. 2010; 26:6804–6808. [PubMed: 20085331]

Dharuman V, Chang BY, Park SM, Hahn JH. Biosens. Bioelectron. 2010; 25:2129–2134. [PubMed: 20303736]

Dharuman V, Hahn JH. Biosens. Bioelectron. 2008; 23:1250–1258. [PubMed: 18187315]

Herne TM, Tarlov MJ. J. Am. Chem. Soc. 1997; 119:8916–8920.

Janek RP, Fawcett WR, Ulman A. Langmuir. 1998; 14:3011–3018.

Keighley SD, Li P, Estrela P, Mighorato P. Biosens. Bioelectron. 2008; 23:1291–1297. [PubMed: 18178423]

Lao RJ, Song SP, Wu HP, Wang LH, Zhang ZZ, He L, Fan CH. Anal. Chem. 2005; 77:6475–6480. [PubMed: 16194115]

Levicky R, Herne TM, Tarlov MJ, Satija SK. J. Am. Chem. Soc. 1998; 120:9787–9792.

Leung TYB, Gerstenberg MC, Lavrich DJ, Scoles G, Schreiber F, Poirier GE. Langmuir. 2000; 16:549–561.

Miranda-Castro R, de-los-Santos-Alvarez N, Lobo-Castanon MJ, Miranda-Ordieres AJ, Tunon-Blanco P. Electroanalysis. 2009; 21:2077–2090.

Park SM, Yoo JS. Anal. Chem. 2003; 75:455A–461A.

Patterson A, Caprio F, Vallee-Belisle A, Moscone D, Plaxco KW, Palleschi G, Ricci F. Anal. Chem. 2010; 82:9109–9115.

Pei H, Lu N, Wen Y, Song S, Liu Y, Yan H, Fan C. Advanced Materials. 2010; 22:4754–4758. [PubMed: 20839255]

Piela B, Wrona PK. J. Electroanal. Chem. 1995; 388:69–79.

Sadik OA, Aluoch AO, Zhou AL. Biosens. Bioelectron. 2009; 24:2749–2765. [PubMed: 19054662]

Sassolas A, Leca-Bouvier BD, Blum LJ. Chem. Rev. 2008; 108:109–139. [PubMed: 18095717]

Steel AB, Herne TM, Tarlov MJ. Anal. Chem. 1998; 70:4670–4677. [PubMed: 9844566]

Steel AB, Levicky RL, Herne TM, Tarlov MJ. Biophys. J. 2000; 79:975–981. [PubMed: 10920027]

Tosar JP, Brañas G, Laíz J. Biosens. Bioelectron. 2010; 26:1205–1217. [PubMed: 20855190]

Wang J. Biosens. Bioelectron. 2006; 21:1887–1892. [PubMed: 16330202]

Wu J, Campuzano S, Halford C, Haake DA, Wang J. Anal. Chem. 2010; 82:8830–8837.

Xia F, White RJ, Zuo XL, Patterson A, Xiao Y, Kang D, Gong X, Plaxco KW, Heeger AJ. J. Am. Chem. Soc. 2010; 132:14346–14348. [PubMed: 20873767]

Zhang J, Lao RJ, Song SP, Yan ZY, Fan CH. Anal. Chem. 2008; 80:9029–9033. [PubMed: 19551931]

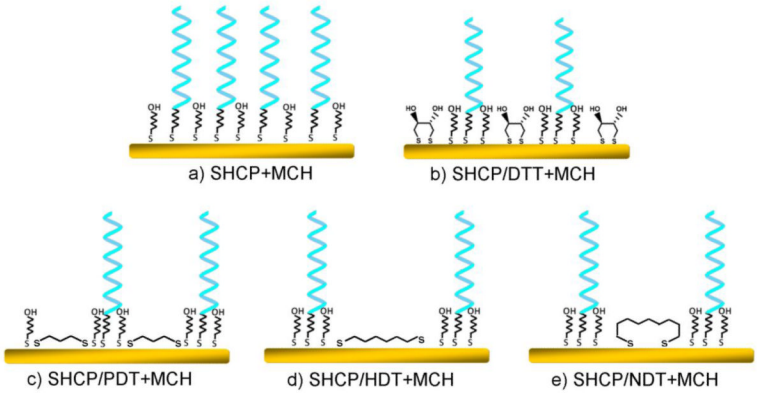

Fig. 1.

DNA recognition interfaces used in this study. Conventional binary SHCP+MCH (a) and ternary SHCP/dithiol+MCH (b-e) monolayers involving DTT (b) or linear dithiols of different lengths: PDT (c), HDT (d), and NDT (e). (Note that these are schematic simplified presentations that do not represent the exact structure of these monolayers).

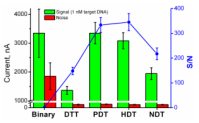

Fig. 2.

Comparative hybridization efficiency, background noise and S/N characteristics for 1 nM target DNA in HB using the different DNA recognition interfaces. Error bars were estimated from five parallel experiments.

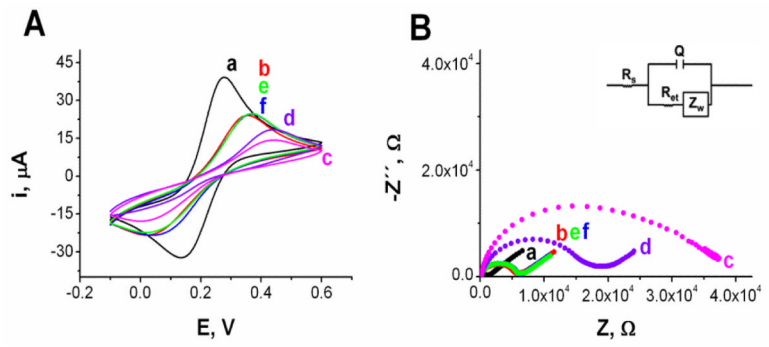

Fig. 3.

(A) Cyclic voltammograms and (B) Nyquist plots (Z″ *vs* Z′) for the faradaic impedance measurements obtained with a bare Au surface (a, black) and with a AuE modified with SHCP+MCH (b, red), SHCP/DTT+MCH (c, pink), SHCP/PDT+MCH (d, purple), SHCP/HDT+MCH (e, green) and SHCP/NDT+MCH (f, blue). Inset in B shows the Randles equivalent used to model the electrochemical impedance spectroscopy data. Parameters: EIS, 5 mM $[Fe(CN)_6]^{3-/4-}$ (1:1) in 0.1 M KCl, 0.01–10,000 Hz frequency range with a 0.01 V r.m.s. signal at +0.25 V (*vs.* Ag/AgCl); CV, v = 100 mV s^{-1}.

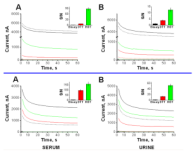

Fig. 4.

(Top, A,B) Performance of the different monolayers tested in 100 % of clinical samples and (Bottom, A,B) non-fouling properties after 24 h immersion in 100 % of clinical samples. Chronoamperometric signals obtained for 1 nM (solid lines) and 0 nM (dotted lines) target DNA. Inset: S/N obtained for 1 nM of target DNA. Data obtained in 100 % of human serum (A) and 100 % of human urine (B). Error bars were estimated from five parallel experiments. Monolayers: SHCP+MCH (black), SHCP/DTT+MCH (red) and SHCP/HDT +MCH (green).

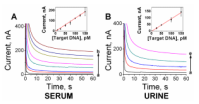

Fig. 5.

Chronoamperometric responses for different target DNA concentrations obtained with the hybridization in untreated and undiluted human serum (A, (a) 0, (b) 10, (c) 25, (d) 50, (e) 75, (f) 100, (g) 125 and (h) 150 pM target DNA) and human urine (B, (a) 0, (b) 25, (c) 50, (d) 100 and (e) 150 pM target DNA). Insets represent the calibration plots obtained in the same range of concentrations after background substraction. Error bars were estimated from five parallel experiments.

Table 1

Electrochemical impedance data for different SAMs. Data were calculated using Randles equivalent circuit

Surface	Q (μF)	Z_W ($\Omega \cdot s^{-1/2}$)	R_{et} (Ω)	θ_{IS}^{R}
Bare	4.96	4.79×10^{-4}	1,029.6	—
SHCP+MCH	0.398	4.43×10^{-4}	5,562.8	0.8149
SHCP/DTT+MCH	0.637	4.03×10^{-4}	32,595.9	0.9684
SHCP/PDT+MCH	0.396	3.77×10^{-4}	17,268.2	0.9404
SHCP/HDT+MCH	0.335	5.30×10^{-4}	5,914.6	0.8259
SHCP/NDT+MCH	0.332	5.40×10^{-4}	5,764.6	0.8234
SHCP/HMT+MCH	0.162	5.56×10^{-4}	2,847.9	0.6385
SHCP/HDT	0.234	6.15×10^{-4}	1,599.8	0.6436